Available online at www.CivileJournal.org

Civil Engineering Journal

(E-ISSN: 2476-3055; ISSN: 2676-6957)

Vol. 11, No. 02, February, 2025

A Study of Biomass Concrete Reinforced with Fiber Composites to Enhance Impact Load Capacity

Kunanon Sakkampang [1, 2], Piyorus Tasenhog [2, 3*], Nirut Onsalung [1, 2], Narong Huchaiyaphum [1]

[1] *Department of Mechanical Engineering, Faculty of Industry and Technology, Rajamangala University of Technology Isan Sakon Nakhon Campus, Thailand.*

[2] *The Material's Impact Resistance Testing Research Unit (Mat-Pact Unit), Faculty of Industry and Technology, Rajamangala University of Technology Isan Sakon Nakhon Campus, Thailand.*

[3] *Department of Civil Engineering, Faculty of Industry and Technology, Rajamangala University of Technology Isan Sakon Nakhon Campus, Thailand.*

Received 17 September 2024; Revised 13 January 2025; Accepted 18 January 2025; Published 01 February 2025

Abstract

This research investigates the energy absorption from impact forces of steel reinforced concrete using fly ash obtained from agricultural processes, reinforced with glass fiber-reinforced polymer (GFRP) bars, compared to steel reinforcement. The reinforcement pattern involves incorporating GFRP bars into a square grid pattern of 4, 9, and 12 openings within bio-steel concrete with dimensions (W × L × H) of 40 × 40 × 10 cm. The testing is conducted using a Drop Test impact testing machine with a 30 kg hammer head at a velocity of 7 m/s, employing two different hammer head configurations: flat and 45-degree angled, to study energy absorption (E_a), specific energy absorption (E_s), and the pattern of deformation resulting from impacts. The study finds that CBRHA-10-fiber A concrete exhibits higher energy absorption and specific energy absorption compared to steel-reinforced (CBRHA-10-steel A) concrete in the same configuration by 18.82% and 26.83%, respectively, in the flat-headed hammer impact configuration. Similarly, in the 45-degree angled hammer head configuration, CBRHA-10-fiber A concrete demonstrates superior energy absorption and specific energy absorption compared to steel reinforcement in the same configuration by 6.10% and 14.92%, respectively. In conclusion, bio-steel reinforced concrete with glass fiber-reinforced polymer (GRFP) reinforcement exhibits good load-bearing capacity and suitability as an alternative to steel reinforcement in future applications.

Keywords: Biomass Concrete; Glass Fiber-Reinforced Polymer (GRFP); Energy Absorption; Specific Energy Absorption.

1. Introduction

The continuous development in the global construction industry highlights the importance of concrete as a primary material for foundational structures worldwide [1-3]. This reliance on concrete is evident in its steadily increasing demand, with primary materials expected to rise to nearly 1.5 billion tons by 2024 [4]. Concrete is extensively used in industrial applications, particularly for factory flooring, which facilitates the movement of heavy machinery and cargo. However, these industrial settings introduce significant challenges to flooring structures, affecting their durability and incurring substantial repair costs [5]. Conventional concrete reinforced with steel rebars can withstand high compressive forces, but it remains vulnerable to damage from dynamic and impact loads caused by collisions with heavy machinery [6].

* Corresponding author: piyoros.ta@rmuti.ac.th

http://dx.doi.org/10.28991/CEJ-2025-011-02-020

The impact resistance of concrete is a critical focus in modern structural engineering, particularly for applications requiring high durability under dynamic loads. To address the limitations of conventional concrete, fiber-reinforced concrete (FRC) has emerged as a promising alternative. FRC exhibits superior energy absorption and dissipation capabilities under impact conditions. Studies by Yoon & Banthia [6] emphasized substantial improvements in crack resistance and energy absorption achieved through the inclusion of fibers. These studies highlighted that the type, volume fraction, and distribution of fibers significantly influence the resistance of concrete to dynamic loads. Recent research by Wang et al. [7] and Murali et al. [8] further explored FRC's performance under lateral and drop-weight impacts, showcasing the effectiveness of hybrid fiber systems—such as carbon nanofibers and polyvinyl alcohol (PVA) fibers—in enhancing abrasion and impact resistance. Additionally, Murali et al. emphasized the critical role of fiber volume in increasing fracture toughness and impact strength, particularly in industrial and seismic environments. The energy absorption capacity of concrete, defined as its ability to withstand deformation under dynamic loading, is another area of significant research. High-performance materials like carbon nanofibers, PVA fibers, and glass fibers enhance the ductility of concrete, enabling it to deform without catastrophic failure. For example, Ji et al. [9] analyzed energy absorption mechanisms using biomimetic spider web structures, demonstrating the importance of lattice designs in distributing and dissipating impact forces. Similarly, Han et al. [10] explored hexagonal lattice structures, which simultaneously improve strength and energy absorption. Comprehensive studies by Gharehbaghi & Farrokhabadi [11] further revealed that strategic material layering in bi-material lattice structures enhances energy absorption while maintaining structural integrity under extreme conditions. These findings provide critical insights for designing fiber-reinforced concrete capable of withstanding both static and dynamic stresses.

In parallel with technological advancements, the integration of sustainable materials has gained momentum in the construction industry to address environmental concerns and resource limitations. The use of waste materials from industries and agriculture to replace conventional cementitious components is increasingly important [12-16]. Among these, rice husk ash (RHA) has gained significant attention as a sustainable alternative. A by-product of rice milling, RHA is rich in silica and pozzolanic properties, making it a valuable component for enhancing concrete performance. Studies by Venkatanarayanan & Rangaraju [17] have shown that replacing 15-30% of cement with RHA can improve concrete's durability, compressive strength, and resistance to chloride ion penetration while reducing permeability. Additionally, Liu et al. [12] emphasized the dual benefits of mitigating environmental pollution and improving concrete's mechanical properties. Furthermore, Beltrán et al. [18] and Lim et al. [19] observed improved workability and long-term compressive strength in RHA concrete, making it suitable for structural and non-structural applications. Feng et al. [20] and Padhi et al. [21] highlighted RHA's lightweight nature and high silica content, which contribute to better thermal insulation and crack resistance. These findings underscore the potential of biomass concrete, particularly with RHA, as a viable solution for developing sustainable and durable construction materials.

The construction industry's shift toward environmentally friendly materials extends to biomass ash, derived from agricultural waste. In regions such as Southeast Asia, agricultural by-products are abundant and serve as primary raw materials [17, 19, 20, 22]. Biomass ash, a waste product from combustion processes, presents environmental concerns but also offers opportunities for sustainable construction. Among these materials, black ash, derived from biomass combustion, is particularly noteworthy. Its lightweight properties and superior physical attributes compared to white ash result from its more complete combustion process. Black ash, with a high SiO_2 content of up to 70%, shows significant potential for pozzolanic reactions [23-26]. Studies indicate that black ash enhances compressive strength when used in optimal proportions. Concrete mixtures incorporating 15-40% biomass ash have demonstrated comparable or improved performance to conventional concrete after 30-60 days of curing [27-31]. However, adherence to design standards is crucial to ensure that the internal structure of conventional concrete remains unaltered for practical construction applications.

Simultaneously, advancements in reinforcement materials have introduced Glass Fiber Reinforced Polymer (GFRP) bars as a sustainable alternative to steel reinforcement in concrete structures. GFRP bars offer superior mechanical properties, including higher tensile strength, excellent energy absorption, and resistance to corrosion. Comparative studies by Patil and Prakash [32] demonstrated that GFRP bars surpass steel in tensile strength, enabling higher energy absorption while maintaining structural integrity. Nematzadeh & Fallah-Valukolaee [33] emphasized the effective bonding behavior of GFRP bars with concrete, enhanced through surface treatments and innovative anchoring systems. Yoo et al. [34, 35] highlighted the superior flexural behavior and reduced environmental degradation of GFRP-reinforced concrete, making it ideal for harsh environments. Additionally, Sijavandi et al. [36] confirmed the higher load-bearing capacity and ductility of GFRP-reinforced concrete under both static and dynamic loads compared to steel. These properties establish GFRP as a suitable choice for lightweight, high-performance materials with extended service life, particularly in industrial flooring applications.

Recent research has highlighted the potential of combining fiber reinforcement with biomass-based concrete to meet the dual goals of sustainability and durability. Studies on mixing black ash with cement suggest that proportions should

not exceed 30% by weight to balance mechanical strength and environmental benefits. The integration of agricultural pozzolanic materials, particularly RHA and black ash, provides a viable pathway to address both environmental and structural challenges in the construction sector. By reducing cement usage, these materials contribute to lower carbon emissions and improved thermal performance. Enhanced testing methodologies are needed to validate these composites under realistic industrial conditions, ensuring their role as next-generation construction materials.

The theoretical foundation of this research integrates principles from material science, structural engineering, and sustainability. Central to the study is the application of composite material theory, which explains the synergistic interaction of different materials to enhance structural performance. For example, FRC leverages fibers to bridge microcracks, improving tensile strength and energy dissipation during dynamic loading. Research by Banthia & Gupta [37] highlighted this bridging mechanism as instrumental in mitigating crack propagation under high-impact conditions. The pozzolanic reaction theory underpins the use of biomass ash as a partial cement replacement. Silica-rich by-products like RHA react with calcium hydroxide in cement to form additional calcium silicate hydrate (C-S-H), the primary binder responsible for concrete's strength Celik et al. [38, 39] emphasized that this reaction enhances durability, strength, and resistance to chemical attacks, aligning well with industrial requirements.

The adoption of GFRP bars is grounded in advanced composite theory, which highlights the advantages of combining lightweight [40-43], high-tensile materials [44-48] with polymer matrices to achieve superior mechanical performance. ACI 440.1R-15 emphasizes GFRP's utility in environments where steel reinforcement faces degradation challenges. Additionally, Kotynia et al. [40] demonstrated that GFRP-reinforced concrete exhibits superior flexural and impact resistance compared to steel reinforcements. By integrating these theoretical frameworks, this study aims to contribute to the development of sustainable, high-performance construction materials capable of meeting modern industrial demands. This study presents an exploration of the characteristics of biomass concrete and GFRP bars, focusing on their preparation and reinforcement design. This is followed by a detailed description of the testing methodology, including compressive strength and impact resistance evaluations. The results of the impact tests are then presented, with an in-depth analysis of the performance of fiber- and steel-reinforced concrete under varying conditions. Finally, the study concludes with a summary of findings and recommendations for future research.

2. Characteristics of Biomass Concrete and Glass Fiber Reinforced Polymer (GFRP)

2.1. Biomass Concrete from Black Ash

The approach for determining the proportion of biomass concrete used in this research is illustrated in Figure 1. It begins with utilizing black ash waste from rice husk combustion industries as a sample with consistent physical characteristics. The black ash is incinerated at temperatures of 500-700°C [49-51] for 23-24 hours and allowed to cool to ambient temperature for another 24 hours. Subsequently, it is finely ground using a grinder for 4 hours and then sieved through a No. 325 sieve with a mesh size of 0.045 mm to check for fineness. If the ground black ash residue in the sieve does not exceed 34%, it is considered suitable for mixing with cement.

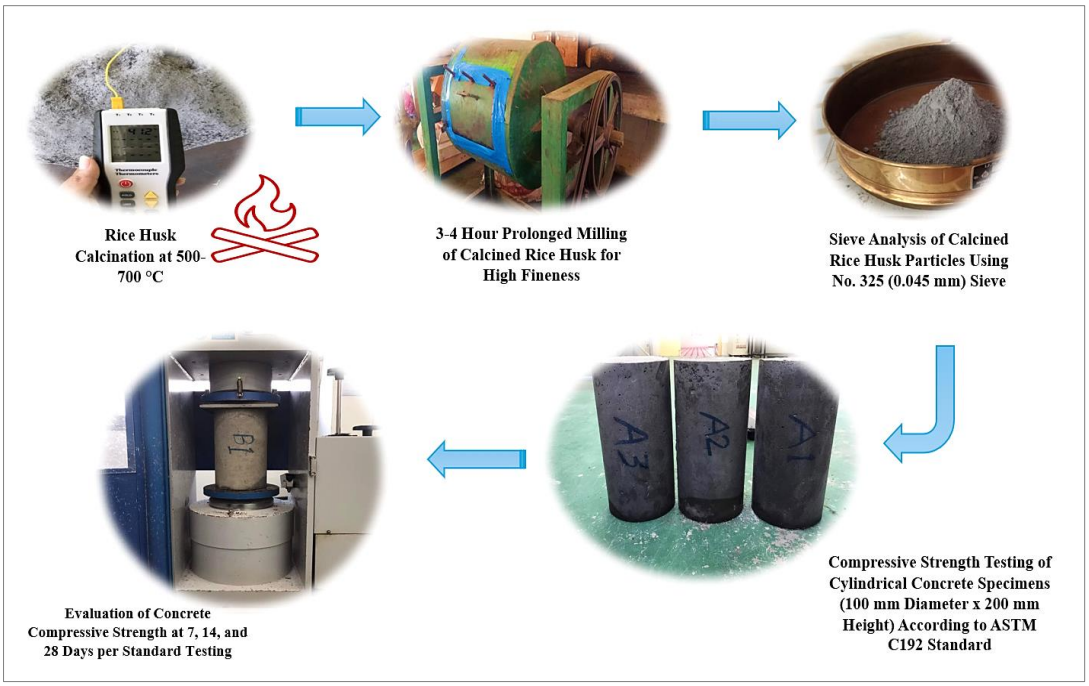

Figure 1. The process of molding and testing biomass concrete from burnt black ash

In the mixture proportions of biomass concrete to determine the appropriate ratio between black ash and cement in this research, the concrete specimens with a compressive strength of 300 kg/cm² were tested according to the ASTM C192 concrete testing standard. The specimens were molded into cylindrical shapes with a diameter of 10 cm and a height of 20 cm at the age of 28 days [52, 53]. These concrete specimens are commonly used in general structural works, with the slump value of the concrete set at 10 ± 2.5 cm. The method for calculating the proportions of concrete mixtures follows the unit weight method, with a unit weight of 12.266 kg, in accordance with the American Concrete Institute (ACI) standards [54, 55]. In this research, the concrete mixture proportions used an upper limit of 20% black ash by weight [56-59]. The researchers increased the proportion of black ash by an additional 5% by weight of the aggregate material, as shown in Table 1.

Table 1. Concrete mixture according to American Concrete Institute (ACI) calculation

Type of Concrete	Percentage replacement by weight	Material (g.)				
		PC	BRHA	Sand	Stone	Water
CPC*	0	214.5	0	419.6	457.2	135.1
CBRHA-10	10	193.1	21.415	419.6	457.2	135.1
CBRHA-15	15	171.6	42.9	419.6	457.2	135.1
CBRHA-20	20	150.2	64.37	419.6	457.2	135.1

Note: * = CPC: Controlled Permeability Concrete, which uses cement as a binder material

The compressive strength testing according to ASTM C192 standard will be conducted after the material is formed into four mixing ratios: CPC, CBRHA-10, CBRHA-15, and CBRHA-20, respectively. The compressive strength will be tested using a 500 kN compression testing machine at 7, 14, and 28 days in accordance with Rahimi et al. [60] and Al-Amoudi et al. [61]. Figure 2, the compressive strength trend of biomass concrete in all four samples shows that using a higher proportion of fly ash as a component in cement will decrease the compressive strength trend of the mixed cement specimens. This is because the amount of fly ash replaces that of the cement, thereby reducing the bonding ability between cement molecules. Additionally, fly ash has lower density, so increasing the proportion of fly ash will decrease the compressive strength. When comparing the proportions of fly ash, it is found that using 10% fly ash results in a compressive strength of 304.50 kgf/cm^2 at 28 days according to ASTM C39 standard. Therefore, this ratio was selected for sample preparation, where rectangular biomass concrete specimens measuring 40×40×10 cm will be created for impact resistance testing and to study the material's energy absorption capabilities.

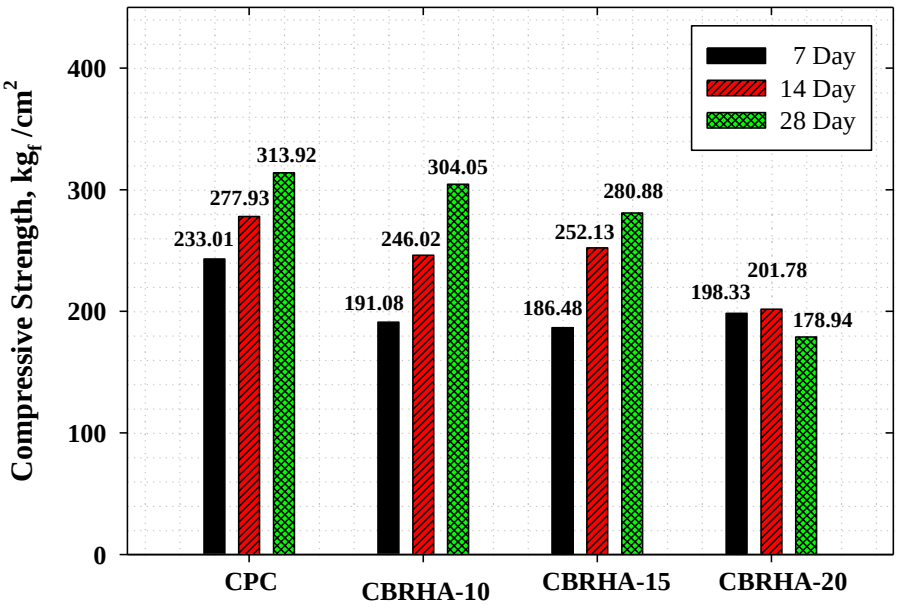

Figure 2. Graph showing the relationship between the compressive strength of biomass concrete at different mixing ratios

2.2. Reinforcement Patterns of GFRP Bars

The GFRP (Glass Fiber Reinforced Polymer) bars used in this research exhibit similar characteristics to steel rebars, which are rod-shaped with spiraled ridges around them, resembling the research conducted by Kotynia et al. [40] and Sanfeng Liu et al. [62], as shown in Figure 3. The tested GFRP bar, with a diameter of 9 cm, demonstrates a tensile strength of 840.91 MPa, a density of 0.061 kgf/cm^2, and a modulus of elasticity of 45 GPa. Table 2 compares the properties of GFRP bars with those of steel used in the testing, revealing that GFRP exhibits higher tensile strength despite its lower density. Therefore, using GFRP for reinforcement in concrete yields better results compared to conventional steel reinforcement. Additionally, it's noteworthy that the modulus of elasticity of GFRP is lower than that of steel, primarily because GFRP is made from glass fibers, resulting in lower elasticity values [63-65].

Figure 3. Configuration of the GFRP Bar Used in the Research Study

Table 2. Comparison of Mechanical Properties between GFRP Bars and Steel Used in Testing

Material	Dimeter (mm.)	Density (kg/m^3)	The tensile strength (MPa)	Modulas of Elasticity (GPa)	Failure for torsion (kgf)
GRFP	9	2002.30	840.91	45	6,830
Steel	9	8089.32	517	200	-

Due to the focus of this research on designing concrete for use as flooring in industrial facilities to withstand impacts, the reinforcement pattern of the GFRP bars in the biomass concrete was designed to have a grid-like configuration with a spacing of 3 cm between each opening, as depicted in Figure 4. Each pattern specifies a gap of 8.5, 11.5, 17.0 cm. Similarly, the reinforcement steel was used in the same configuration to facilitate comparison of experimental results.

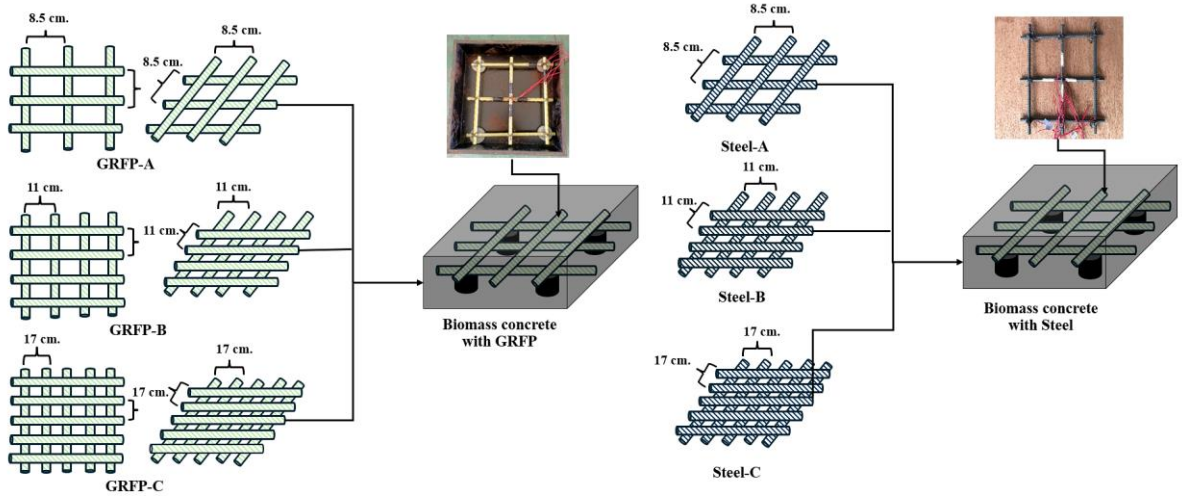

Figure 4. the reinforcement patterns of both the GFRP bars and the steel bars in the biomass concrete

3. Impact Testing

In this research, impact testing of the biomass concrete reinforced with GFRP bars will be conducted. The testing setup will consist of a 3-meter tall column (V=7.67 m/s) designed to release a freely falling hammer head to impact the material under test, similar to the studies conducted by Jun Wang et al. [7], Yang et al. [66], and Murali et al. [8], as

depicted in Figure 5. The hammer head will be of conical shape with a flat contact surface and a sharp 45° angle to examine the differences between full-face and partial-face impacts. Both types of hammer heads will have a weight of 30 kg. The test specimens will be designed to be placed on a support base to allow for controlled bending during impact. Load cells will be installed at the base of the test setup to measure the load generated by the impact. Additionally, LVDTs will be installed at the bottom of the concrete specimens to measure the deflection when impacted. The hammer weight and velocity were selected to represent the minimum threshold values necessary to induce observable damage to the specimens. This ensured the progression of damage patterns could be studied without causing catastrophic failure, enabling a detailed analysis of energy dissipation and specific energy absorption. The configurations of flat and angular hammer heads were chosen to simulate real-world industrial impact scenarios. By using the smallest values capable of causing noticeable damage, the study captures the early stages of material failure, allowing for precise evaluation of energy absorption and crack propagation. The analysis of the experimental results regarding the energy absorption capacity and specific energy absorption will be calculated using Equations 1 and 2 [9-11].

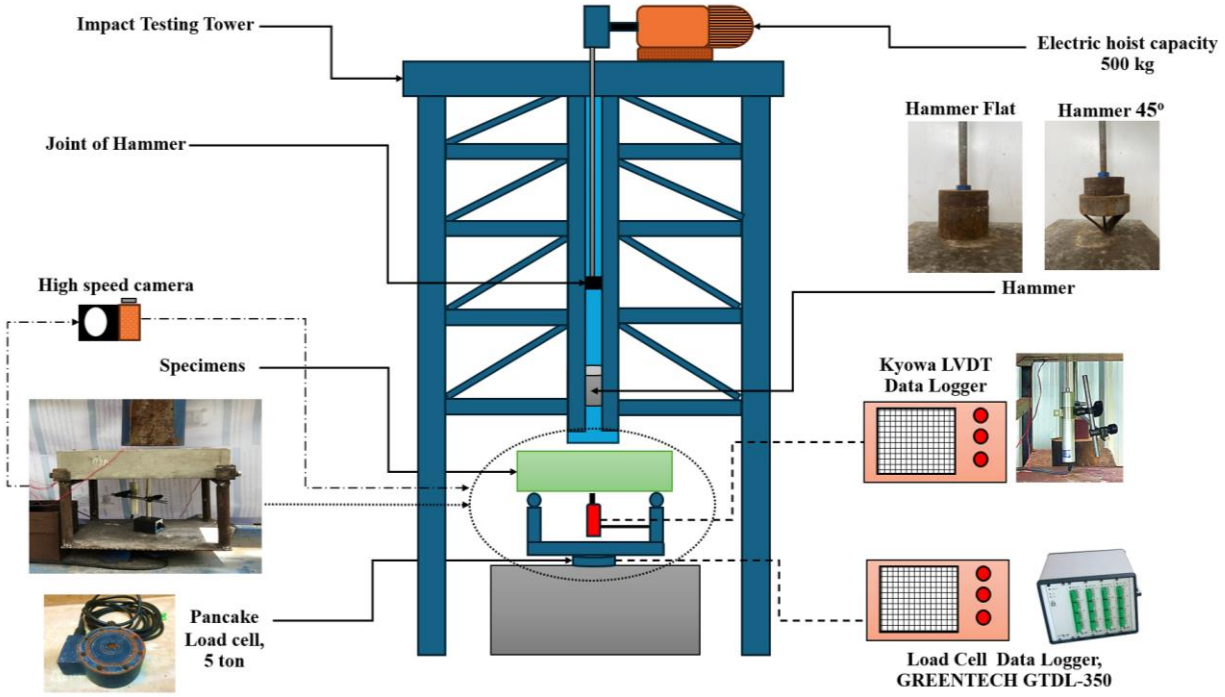

Figure 5. Impact testing machine used in the experimental study

$$E_a = P_{mean}.S = \int PdS \quad (1)$$

$$E_s = \frac{P_{mean}.S}{mass} \quad (2)$$

When E_a is the energy absorption, E_s is the specific energy absorption, P_{mean} is the average load, S is the distance the specimen deflects from the beginning to the end point, P is the load applied to the specimen, and ds is the deflection of the specimen.

4. Results and Discussion

4.1. Load and Average Load of Biomass Fiber-Reinforced Concrete Using Flat-Anvil Hammer

The results of the impact test on biofiber-reinforced concrete specimens using a flat-ended piston, as recorded from load cells in Figure 6, show that the load curves of biofiber-reinforced concrete in each configuration are closely comparable. The maximum load of biofiber-reinforced concrete using CBRHA-10-fiber A is 17.29 kN, which is lower than the maximum load of the same configuration reinforced with steel (CBRHA-10-Steel A) at 18.21 kN. This difference can be attributed to the transmission of force from the impacting piston onto the material; if the material absorbs the force well, the load value decreases. Considering Figure 6-A, it is evident that the load of concrete reinforced with steel is higher compared to that reinforced with fiber bars when comparing the same quantity of steel and fiber. Moreover, from Figure 7-B, the average load of concrete reinforced with CBRHA-10-fiber A, CBRHA-10-fiber B, and CBRHA-10-fiber C is 8.33, 8.40, and 7.48 kN, respectively. This average load analysis will be used to calculate energy absorption (E_a) and specific energy absorption (E_s) subsequently. Another parameter considered in assessing energy absorption and specific energy absorption is the deflection obtained from LVDT data collection.

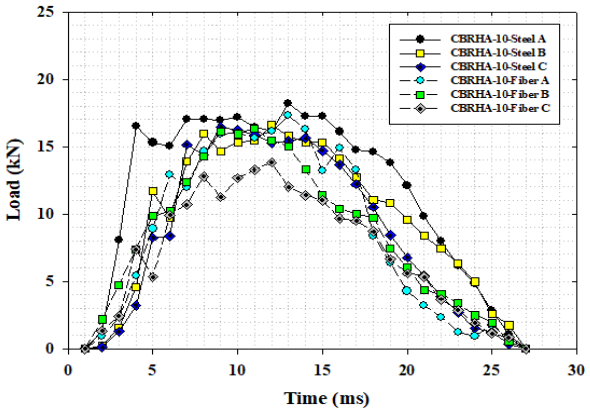

(a)

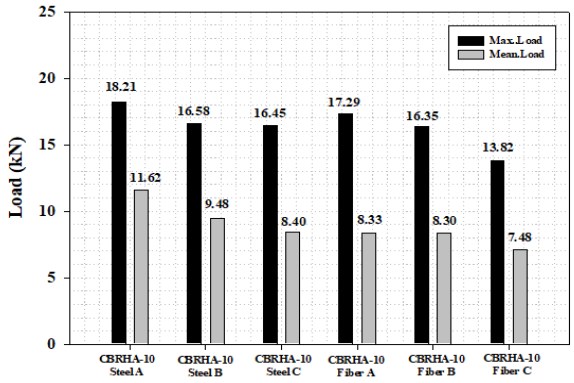

(b)

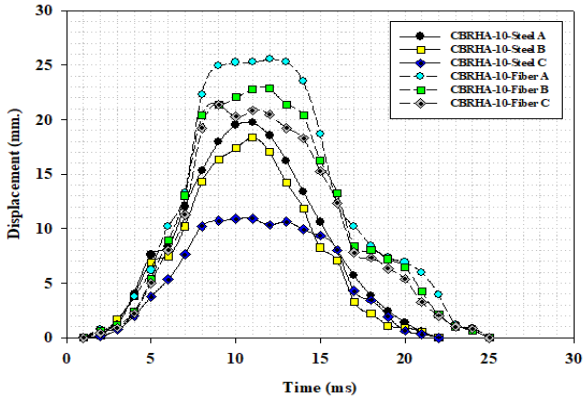

(c)

Figure 6. Impact test results of biomass fiber-reinforced concrete using flat-anvil hammer,)A) Graph showing the relationship between load and time of biomass fiber-reinforced concrete using steel and fiber bars when subjected to impact using a flat-anvil hammer,)B) Graph depicting the maximum load and average load of biomass fiber-reinforced concrete using steel and fiber bars when subjected to impact using a flat-anvil hammer,)C) Graph illustrating the relationship between deflection and time of biomass fiber-reinforced concrete using steel and fiber bars when subjected to impact using a flat-anvil hammer.

To better understand these behaviors, the study provides a detailed examination of the GFRP reinforcement grid patterns and their impact on performance under impact load conditions. The grid patterns are specified with gaps of 8.5 cm, 11 cm, and 17 cm, corresponding to cross-sectional area ratios of 0.0047, 0.0063, and 0.0079, respectively. These variations in reinforcement density significantly influence the behavior of the concrete slabs. Denser grids, such as the 8.5 cm pattern, demonstrate superior performance in terms of energy absorption and specific energy absorption, effectively dissipating impact energy and minimizing damage. Conversely, wider grid patterns show lower energy dissipation capacity and greater deformation under similar conditions. The study evaluates the slabs' impact load capacity, energy absorption, and damage characteristics using different hammer configurations, including flat and angular impacts. The results reveal that denser reinforcement provides better resistance to impact loads, with a noticeable improvement in structural integrity. However, the study also highlights the need for considering trade-offs, such as material costs and potential effects on long-term durability, when selecting reinforcement densities for practical applications.

This improved understanding of the reinforcement grid's role aligns with the higher deflection values observed in fiber-reinforced concrete specimens compared to their steel-reinforced counterparts. Fiber materials enhance the flexibility of the concrete matrix, as reflected in higher deflection values of 25.5188, 22.8475, and 20.8364 mm for CBRHA-10-fiber A, CBRHA-10-fiber B, and CBRHA-10-fiber C, respectively. This increased flexibility contributes to greater energy dissipation under impact loads. In contrast, the lower deflection values of CBRHA-10-Steel A (19.7024 mm), CBRHA-10-Steel B (18.3636 mm), and CBRHA-10-Steel C (10.9223 mm) highlight the rigidity and limited deformation capacity of steel reinforcement. These findings underscore the role of fiber reinforcement in enhancing impact resilience through improved energy absorption and deformation capacity.

Examining the graph in Figure 6-C, the deflection values during impact reveal that the deflection of concrete reinforced with fiber bars is relatively higher than that of steel reinforcement. CBRHA-10-fiber A, CBRHA-10-fiber B, and CBRHA-10-fiber C have deflection values of 25.5188, 22.8475, and 20.8364 mm, respectively. On the other hand, CBRHA-10-Steel A, CBRHA-10-Steel B, and CBRHA-10-Steel C exhibit maximum deflection values of 19.7024, 18.3636, and 10.9223 mm, respectively. These higher deflection values in fiber-reinforced specimens occur due to the increased flexibility provided by the fiber materials, which enhance the concrete matrix's ability to dissipate impact forces. In contrast, steel-reinforced specimens, due to their rigidity, show less deflection and higher susceptibility to localized stress concentrations.

Therefore, it is essential to design the fiber reinforcement pattern appropriately before implementation. This design consideration directly impacts the material's flexibility, improving its ability to withstand impact and resulting in increased energy absorption. These findings emphasize the importance of optimizing reinforcement patterns to achieve the desired balance between performance, cost-effectiveness, and long-term durability in practical applications.

4.2. Load and Average Load of Biofiber-Reinforced Concrete Using 45-Degree Angular Hammer

The study of the impact of angular-ended pistons, as depicted in Figure 7(A), reveals that the load values for the 45-degree angular-ended piston are higher when compared to those obtained using flat-ended pistons. This occurs because the pointed nature of the angular-ended piston results in greater penetration into the material surface, concentrating the mass at the tip of the piston and thereby generating higher localized stress fields. Consequently, this behavior aligns with experiments using flat-ended pistons, where conventional reinforced concrete exhibits higher load values compared to fiber-reinforced concrete.

As shown in Figure 7(B), the maximum load values and average load values for biofiber-reinforced concrete, specifically CBRHA-10-fiber A, CBRHA-10-fiber B, and CBRHA-10-fiber C, are 17.29, 16.35, and 13.82 kN, respectively. Similarly, the average load values for fiber-reinforced concrete are lower compared to conventional reinforced concrete, reflecting trends observed with flat-ended pistons. The incorporation of fiber bars contributes to the reduction in both maximum and average load values, which can be attributed to the distribution of forces facilitated by the fiber reinforcement. These findings are consistent with previous studies on the effect of impact geometry on material behavior. Sharper impact heads, such as the 45-degree angular piston, result in concentrated stress fields that promote localized damage and higher load values. Moreover, the angular shape of the piston head facilitates the initiation and propagation of microcracks through the specimen, creating distinct damage patterns compared to those observed under flat-ended impacts [67-69].

The displacement of specimens under angular-ended piston impacts, illustrated in Figure 7(C), reveals lower displacement values compared to impacts from flat-ended pistons. For instance, CBRHA-10-fiber A, CBRHA-10-fiber B, and CBRHA-10-fiber C exhibit displacement values of 15.2625, 12.1919, and 10.4407 mm, respectively, which are higher than the maximum displacement values observed in CBRHA-10-Steel A, CBRHA-10-Steel B, and CBRHA-10-Steel C, recorded at 12.0999, 10.8282, and 9.5354 mm, respectively. This discrepancy is primarily due to the pointed nature of the angular-ended piston, which reduces the contact area and results in less displacement of the material.

The results of this study emphasize the critical influence of impact geometry on material performance. The comparison between flat and angular impact tests highlights how fiber reinforcement enhances energy dissipation and flexibility under flat impacts, while angular impacts accentuate the inherent trade-offs between flexibility and ultimate load resistance. Such insights are essential for designing tailored reinforcement systems that account for varying impact scenarios in industrial applications, ensuring an optimal balance between performance and material resilience.

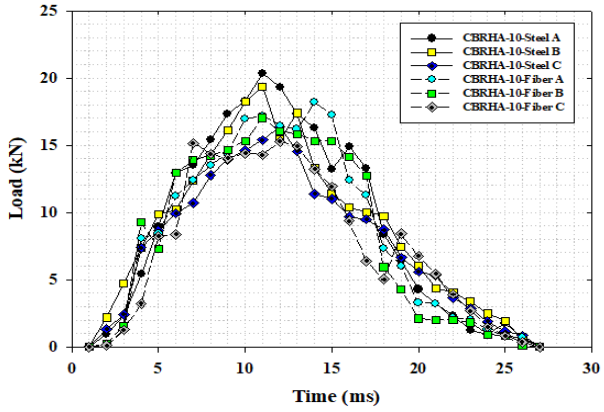

(a)

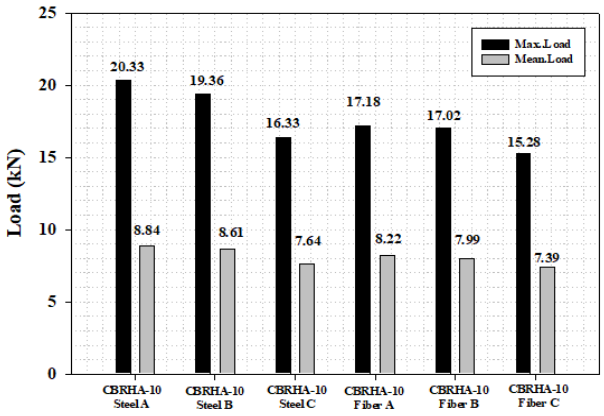

(b)

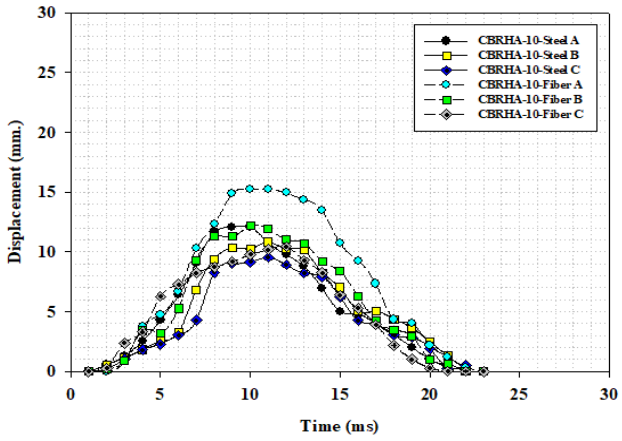

(c)

Figure 7. Impact Testing Results of Biofiber-Reinforced Concrete with Steel and Fiber Bars Using 45-Degree Angular-Ended Piston, (A) Graph depicting the relationship between load and time for biofiber-reinforced concrete with steel and fiber bars when using a 45-degree angular-ended piston, (B) Graph illustrating the maximum load and average load of biofiber-reinforced concrete with steel and fiber bars when using a 45-degree angular-ended piston, (C) Graph showing the relationship between the displacement of the specimen and time for biofiber-reinforced concrete with steel and fiber bars when using a 45-degree angular-ended piston.

4.3. Energy Absorption and Specific Energy Absorption

The analysis of the energy absorption of bio-concrete in various configurations, based on Equations 1 and 2, is presented in the graph in Figure 8. Upon examination of the tests conducted with the flat-headed ram, it is observed that the energy absorption of bio-concrete reinforced with fiber bars, specifically CBRHA-10-fiber A, exhibits the highest value at 0.441 kJ. In comparison, bio-concrete reinforced with fiber bars CBRHA-10-fiber B and CBRHA-10-fiber C also demonstrate higher values than bio-concrete reinforced with steel, despite having similar average load values. This superior performance is attributed to the ability of the fiber bars to enhance the material's compression properties, leading to greater energy dissipation during impact.

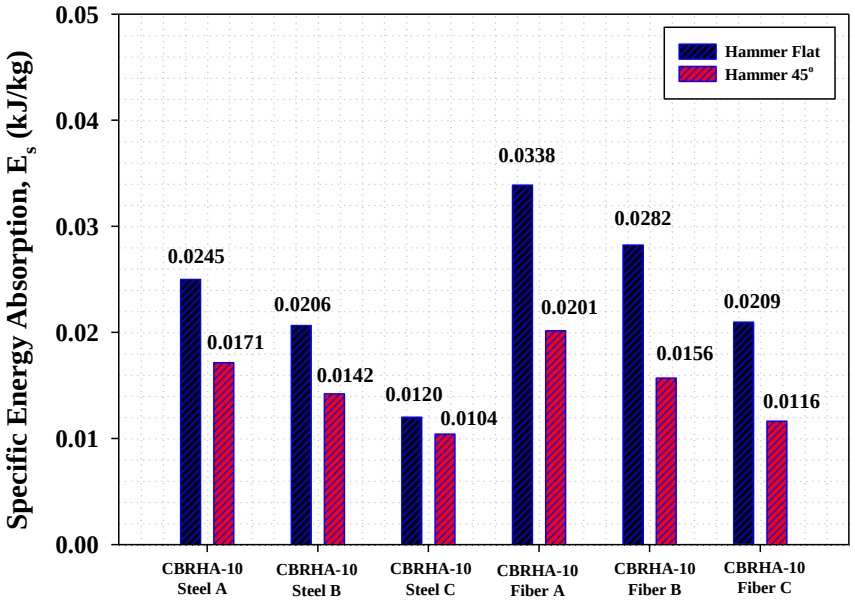

Figure 8. Graph showing the energy absorption values of steel-reinforced and fiber-reinforced biomass-concrete

These findings indicate that the increased energy absorption in fiber-reinforced configurations can be attributed to the distributed load transfer mechanism provided by the fibers. This mechanism facilitates the dissipation of impact energy through the progressive deformation of the matrix, contrasting sharply with the brittle failure behavior commonly observed in steel-reinforced configurations [9, 11]. The fibers' ability to evenly distribute stresses prevents localized damage and contributes to the overall durability and performance of the material.

Similarly, the results obtained with the 45-degree angled ram align with those of the flat-headed ram tests, although with reduced energy absorption values. In this configuration, the energy absorption of CBRHA-10-fiber A registers the highest value at 0.262 kJ. The reduction in energy absorption can be attributed to the increased intensity and concentrated force applied by the angled ram, which leads to greater damage and higher localized loads. Additionally, the minimal compression of the specimens in this configuration contributes to the lower overall energy absorption values. This highlights the influence of impact geometry on the material's behavior under dynamic loading conditions.

The decreased energy absorption under angular impacts underscores the importance of optimizing reinforcement patterns to improve performance in such scenarios. As angular impacts generate more localized damage, reinforcement strategies must focus on enhancing local toughness and crack resistance to mitigate inefficiencies in energy dissipation. Advanced reinforcement geometries and hybrid material integrations, as highlighted in recent studies [10, 33], offer promising approaches to address these challenges and improve the resilience of fiber-reinforced bio-concrete under diverse impact conditions. By tailoring reinforcement strategies to specific impact scenarios, it is possible to achieve a more balanced performance and extend the applications of bio-concrete in demanding environments.

In Figure 9, the analysis results of specific energy absorption of bio-concrete reinforced with steel and fiber bars reveal that the specific energy absorption of fiber-reinforced concrete is higher than that of steel-reinforced concrete. Considering the pattern of impact by the flat-headed probe, it is observed that CBRHA-10-fiber A has the highest specific energy absorption value at 0.0308 kJ/kg, which is higher than that of CBRHA-10-Steel A at 0.0245 kJ/kg. This is attributed to the lightweight nature of fiber bars compared to steel and their superior energy absorption properties. Consistently, when considering the 45-degree angled probe, it is found that fiber-reinforced concrete exhibits higher specific energy absorption. Additionally, it is observed that the specific energy absorption decreases with the angled probe, attributed to the lesser deformation of the specimen, leading to higher transmitted forces, particularly evident in tests with the flat-headed probe. The percentage differences in specific energy absorption between CBRHA-10-fiber A and CBRHA-10-Steel A are 18.82% and 26.33%, respectively, as shown in Table 3. The ratios of steel and fiber reinforcement in other configurations align with CBRHA-10-fiber A, where the results of fiber bar reinforcement consistently demonstrate better Ea and Es values compared to steel reinforcement. Moreover, for tests with the 45-degree angled probe, the differences between steel and fiber reinforcement tend to converge, indicating significant damage due to probe penetration, resulting in decreased impact resistance of fiber bars.

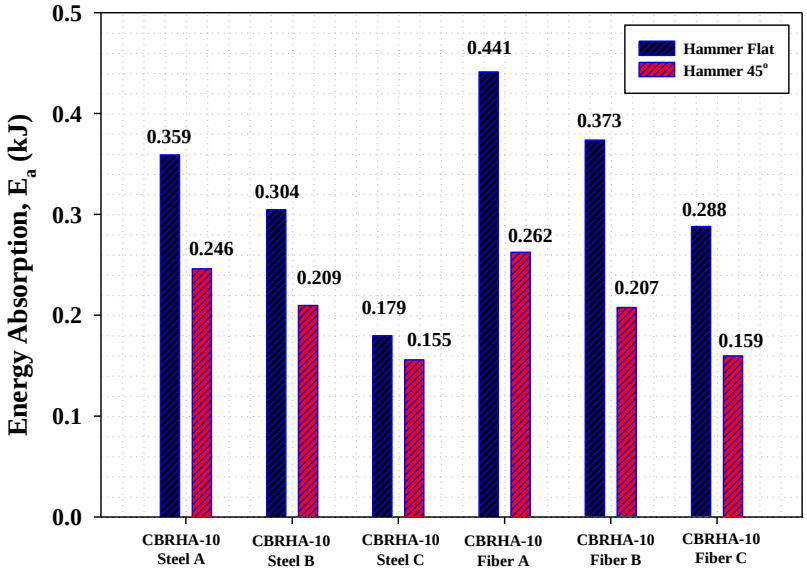

Figure 9. The specific energy absorption values of biomass concrete reinforced with steel and fiber bars

Table 3. the differences in energy absorption and specific energy absorption of concrete reinforced with steel and fiber bars.

	Type	P_{max} (kN)	P_{mean} (kN)	Mass (kg)	S (m)	E_a (kJ)	E_s (kJ/kg)
			Hammer Flat				
	Steel	18.21	11.62	14.36	0.0197	0.359	0.0249
A	CRFP	17.29	8.33	13.02	0.0255	0.441	0.0338
			% Difference			18.82 %	26.33 %
	Steel	16.58	9.48	14.75	0.0183	0.304	0.0206
B	CRFP	16.35	8.30	13.23	0.0228	0.373	0.0282
			% Difference			18.48 %	29.95 %
	Steel	16.45	8.40	14.97	0.0109	0.179	0.0120
C	CRFP	13.82	7.48	13.73	0.0208	0.288	0.0209
			% Difference			37.84 %	42.58 %
			Hammer 45°				
	Steel	20.33	8.84	14.36	0.0120	0.246	0.0171
A	CRFP	17.18	8.22	13.02	0.0152	0.262	0.0201
			% Difference			6.10 %	14.92 %
	Steel	19.36	8.61	14.75	0.0108	0.209	0.0142
B	CRFP	17.02	7.99	13.23	0.0121	0.210	0.0156
			% Difference			0.47 %	8.97 %
	Steel	16.33	7.64	14.97	0.0095	0.155	0.0104
C	CRFP	15.28	7.39	13.73	0.0104	0.159	0.0116
			% Difference			2.51 %	10.34 %

4.4. Damage Characteristics of Bio-Steel and Fiber-Reinforced Concrete from Impact

When examining the damage patterns resulting from impacts with both flat and 45-degree angle hammer heads, as shown in Figure 10, it is observed that damage predominantly occurs at the bottom surface of the specimen. This aligns with findings from various studies that attribute the damage to bending forces, which result in cracks and fissures primarily at the mid-section of the specimen. Upon closer inspection, specimens impacted with flat hammer heads exhibit fewer cracks compared to those impacted with 45-degree angle hammer heads, highlighting the influence of impact geometry on damage characteristics. Both steel and fiber bar reinforcements exhibit similar overall damage patterns, though the extent of damage varies based on the reinforcement type.

Figure 10. The damage patterns from impact on bio-steel and fiber-reinforced concrete using a flat hammer head

The observed variations in crack propagation behavior are consistent with the findings of Mostofinejad et al. [70], which emphasize the significant role of reinforcement type in mitigating crack widths and maintaining the structural integrity of the damaged zones. Fiber reinforcements, in particular, are shown to reduce crack widths and improve the durability of the specimens compared to steel-reinforced configurations. These findings underscore the advantages of fiber reinforcement in enhancing impact resilience.

Selecting reinforcement combinations, such as CBRHA-10-Steel C and CBRHA-10-Fiber C, results in reduced damage due to their higher material incorporation. However, this comes at the cost of increased concrete weight, which can influence specific energy absorption values. While these combinations perform better than other configurations, all three reinforcement patterns exhibit similar levels of damage under certain conditions. For impacts with 45-degree angle hammer heads, damage is notably more severe compared to impacts with flat hammer heads. The concentrated force exerted by the pointed hammer head leads to more extensive and elongated damage patterns, as opposed to the localized indentations caused by flat hammer heads. Despite the superior performance of CBRHA-10-Steel C and CBRHA-10-Fiber C, cracks that render the concrete prone to catastrophic failure are still observed, as seen in configurations such as CBRHA-10-Steel A, CBRHA-10-Steel B, CBRHA-10-Fiber A, and CBRHA-10-Fiber B.

These findings highlight the critical importance of tailored reinforcement strategies to address varying impact scenarios effectively. Integrating hybrid reinforcement systems, combining high-strength fibers with traditional steel, offers a promising solution to enhance performance under severe impact conditions. Recent studies [71, 72] have identified advanced hybrid systems as capable of achieving superior durability and energy absorption. Additionally, advanced modeling techniques are recommended to optimize these reinforcement systems for industrial applications, ensuring that the balance between material performance, cost, and weight is achieved. Additionally, Figure 11 confirms that the use of higher quantities of steel and fiber slightly increases the strength of concrete. Optimal material selection helps in cost-saving and ensures sustainable usage patterns, emphasizing the importance of careful consideration.

Figure 11. depicts the damage patterns from impact on steel-reinforced and fiber-reinforced concrete using a - 45 degree angled hammer head

5. Conclusions

This research investigated the energy absorption characteristics of bio-steel reinforced concrete using fiber-reinforced polymer (FRP) compared to steel reinforcement, simulating scenarios such as industrial floor surfaces where damage may occur from the movement of heavy equipment or machinery in factories. From the study of the properties of bio-steel concrete in various suitable proportions for application, it was found that CBRHA-10 concrete (mixed with 10% by weight of fly ash) exhibited favorable properties for floor design. From compression resistance tests, it was found that CBRHA-10 concrete had a compressive strength of 304.50 Kgf/cm^2 at 28 days of testing, meeting the standards for concrete usage in the country.

In terms of reinforcing materials, when subjected to energy absorption and specific energy absorption tests from impact by a hammer head at a velocity of V=7.67 m/s and a head weight of 30 kg, it was found that in tests using a flat-headed hammer for impact, CBRHA-10-fiber A concrete had the highest values at 0.441 kJ and 0.0308 kJ/kg, respectively. This resulted in significantly higher energy absorption compared to steel-reinforced (CBRHA-10-steel A) concrete in the same configuration, by 18.82% and 26.83%, respectively. Consistent with tests with a 45-degree angled hammer head, CBRHA-10-fiber A concrete exhibited better energy absorption and specific energy absorption compared to steel-reinforced concrete in the same configuration by 6.10% and 14.92%, respectively. Differences in impact between the two types of hammer heads resulted in different damage patterns, with flat-headed hammers causing minimal damage with slight indentation along the bottom edge of the specimen. On the other hand, impacts with a 45-degree angled hammer head resulted in wider damage areas and higher fracture occurrence along the bottom edge of the specimen, characteristic of bending force impact. Therefore, the design and consideration of reinforcing materials, whether steel or fiber bars, should also take into account cost-effectiveness, as excessive material reinforcement leads to unnecessary construction costs.

To contextualize these findings, it is essential to consider the current standards and design practices for industrial flooring, particularly in scenarios requiring high load-bearing capacity. Industrial floor slabs are typically categorized into two main types: ground-supported slabs and pile-supported slabs. Selecting the appropriate type requires careful evaluation by design engineers, particularly considering factors such as plastic shrinkage settlement of the soil, which varies based on soil type. Both floor systems can improve the tensile resistance of the concrete slab through the use of steel mesh reinforcement or fiber-reinforced concrete systems, enhancing the slab's tensile capacity and overall performance. In Thailand, the Ministerial Regulations on Building Control, B.E. 2522 (1979) specify that industrial floors and warehouses must be designed to withstand a minimum live load of 500 kg/m². The exact load requirements, however, are contingent on the specific type of industry and its operations. For example, facilities housing printing factories, heavy machinery, or vibratory equipment may necessitate custom structural designs for certain sections, isolating them from the general industrial flooring to ensure durability and functionality.

Applying bio-steel and fiber-reinforced concrete in industrial applications, particularly for concrete floors in factories handling heavy equipment and machinery, has shown promising results in terms of load-bearing capacity and suitability as an alternative to steel. However, further examination of material integrity is necessary to determine whether fiber-reinforced concrete is more susceptible to degradation compared to steel over prolonged periods. Additionally, the incorporation of biomass fly ash to improve properties for mixing with cement should be explored further to mitigate pollution from cement production and maximize agricultural waste utilization for environmental sustainability.

The study successfully introduces rice husk ash (RHA) and biomass fly ash as sustainable alternatives to traditional cement but does not sufficiently address the variability in these materials' properties. Differences in combustion processes, regional availability, and chemical composition could affect material consistency and performance. Additionally, while the superior energy absorption of biomass concrete with GFRP bars is demonstrated, the study highlights the need for further research on material degradation over time, particularly for GFRP reinforcement under prolonged environmental exposure. The durability of biomass concrete in challenging industrial conditions, such as chemical exposure or extreme temperatures, is also an area requiring more detailed examination. Furthermore, the optimal design parameters, such as variations in GFRP bar spacing, fly ash proportions, and concrete composition, remain underexplored.

The study also does not address scaling challenges for the production of biomass concrete and GFRP bars for widespread industrial application. Discussions on the fatigue performance of these materials under repeated impacts over extended periods are limited, as is the economic feasibility of using biomass concrete reinforced with GFRP on a large scale. To enhance the study's robustness, it would be beneficial to include explicit discussions on material variability and its influence on consistency, long-term durability testing in real-world settings, and the supply chain and cost implications of broader adoption of these sustainable materials. Including these aspects would provide a more comprehensive perspective on the study's findings and applications.

6. Declarations

6.1. Author Contributions

Conceptualization, K.S., P.T., N.O., and N.H.; methodology, K.S. and P.T.; validation, K.S., P.T., and N.O.; formal analysis, K.S., P.T., and N.O.; investigation, K.S., P.T., N.O., and N.H.; resources, K.S., P.T., N.O., and N.H.; data curation, K.S., P.T., N.O., and N.H.; writing—original draft preparation, K.S., P.T., N.O., and N.H.; writing—review and editing, K.S., P.T., N.O., and N.H.; visualization, K.S., P.T., N.O., and N.H.; supervision, K.S., P.T., and N.O.; project administration, K.S.; funding acquisition, K.S., P.T., N.O., and N.H. All authors have read and agreed to the published version of the manuscript.

6.2. Data Availability Statement

The data presented in this study are available in the article.

6.3. Funding and Acknowledgements

The researchers would like to express their gratitude to Rajamangala University of Technology Isan for providing financial support through the Fundamental Fund research grant for the fiscal year 2024, project code FF67/P1-085. The researchers also wish to extend their appreciation to The Material's Impact Resistance Testing Research Unit (Mat-Pact Unit), Faculty of Industry and Technology, Rajamangala University of Technology Isan Sakon Nakhon Campus, for providing equipment support for this research endeavor.

6.4. Conflicts of Interest

The authors declare no conflict of interest.

7. References

[1] Neville, A.M. (2011) Properties of Concrete. Pearson Education Limited, London, United Kingdom.

[2] Smitha, M. P., Suji, D., Shanthi, M., & Adesina, A. (2022). Application of bacterial biomass in biocementation process to enhance the mechanical and durability properties of concrete. Cleaner Materials, 3, 100050. doi:10.1016/j.clema.2022.100050.

[3] Benjamin, B., Zachariah, S., Sudhakumar, J., & Suchithra, T. V. (2024). Harnessing construction biotechnology for sustainable upcycled cement composites: A meta-analytical review. Journal of Building Engineering, 86. doi:10.1016/j.jobe.2024.108973.

[4] Zhou, Z., Wei, Y., Wang, G., Wang, J., Lin, Y., & Zhu, B. (2024). Experimental study on the basic properties of new biomass bamboo aggregate concrete. Journal of Building Engineering, 86, 108892. doi:10.1016/j.jobe.2024.108892.

[5] Trabucchi, I., Tiberti, G., Conforti, A., Medeghini, F., & Plizzari, G. A. (2021). Experimental study on Steel Fiber Reinforced Concrete and Reinforced Concrete elements under concentrated loads. Construction and Building Materials, 307, 124834. doi:10.1016/j.conbuildmat.2021.124834.

[6] Yoo, D. Y., & Banthia, N. (2019). Impact resistance of fiber-reinforced concrete – A review. Cement and Concrete Composites, 104, 103389. doi:10.1016/j.cemconcomp.2019.103389.

[7] Wang, J., Fu, R., & Dong, H. (2023). Carbon nanofibers and PVA fiber hybrid concrete: Abrasion and impact resistance. Journal of Building Engineering, 80, 107894. doi:10.1016/j.jobe.2023.107894.

[8] Murali, G., Katman, H. Y. B., Wong, L. S., Ibrahim, M. R., Ramkumar, V. R., & Abid, S. R. (2023). Effect of recycled lime sludge, calcined clay and silica fume blended binder-based fibrous concrete with superior impact strength and fracture toughness. Construction and Building Materials, 409, 133880. doi:10.1016/j.conbuildmat.2023.133880.

[9] Ji, Y., Gao, Z., Chen, W., Huang, H., Li, M., & Li, X. (2024). Study on the deformation mode and energy absorption characteristics of a corner-enhanced biomimetic spider web hierarchical structure. Thin-Walled Structures, 199, 111810. doi:10.1016/j.tws.2024.111810.

[10] Han, Z., Ma, Z., Tong, S., Shen, G., Sun, Y., Li, J., Zhao, H., & Ren, L. (2024). Simultaneous enhancements of energy absorption and strength driven by hexagonal close-packed lattice structures of resin revealed by in-situ compression. Thin-Walled Structures, 197, 111586. doi:10.1016/j.tws.2024.111586.

[11] Gharehbaghi, H., & Farrokhabadi, A. (2024). Experimental, analytical, and numerical studies of the energy absorption capacity of bi-material lattice structures based on quadrilateral bipyramid unit cell. Composite Structures, 337, 118042. doi:10.1016/j.compstruct.2024.118042.

[12] Liu, H., Li, Q., & Ni, S. (2022). Assessment of the engineering properties of biomass recycled aggregate concrete developed from coconut shells. Construction and Building Materials, 342, 128015. doi:10.1016/j.conbuildmat.2022.128015.

[13] Xiao, J.-Zh., Li, J.-B., & Zhang, Ch. (2006). On relationships between the mechanical properties of recycled aggregate concrete: An overview. Materials and Structures, 39(6), 655–664. doi:10.1617/s11527-006-9093-0.

[14] Radonjanin, V., Malešev, M., Marinković, S., & Al Malty, A. E. S. (2013). Green recycled aggregate concrete. Construction and Building Materials, 47, 1503–1511. doi:10.1016/j.conbuildmat.2013.06.076.

[15] Andreu, G., & Miren, E. (2014). Experimental analysis of properties of high performance recycled aggregate concrete. Construction and Building Materials, 52, 227–235. doi:10.1016/j.conbuildmat.2013.11.054.

[16] Tam, V. W. Y., Butera, A., Le, K. N., & Li, W. (2020). Utilising CO_2 technologies for recycled aggregate concrete: A critical review. Construction and Building Materials, 250, 118903. doi:10.1016/j.conbuildmat.2020.118903.

[17] Venkatanarayanan, H. K., & Rangaraju, P. R. (2013). Material Characterization Studies on Low- and High-Carbon Rice Husk Ash and Their Performance in Portland Cement Mixtures. Advances in Civil Engineering Materials, 2(1), 266–287. doi:10.1520/acem20120056.

[18] Beltrán, M. G., Agrela, F., Barbudo, A., Ayuso, J., & Ramírez, A. (2014). Mechanical and durability properties of concretes manufactured with biomass bottom ash and recycled coarse aggregates. Construction and Building Materials, 72, 231–238. doi:10.1016/j.conbuildmat.2014.09.019.

[19] Lim, J. S., Abdul Manan, Z., Wan Alwi, S. R., & Hashim, H. (2012). A review on utilisation of biomass from rice industry as a source of renewable energy. Renewable and Sustainable Energy Reviews, 16(5), 3084–3094. doi:10.1016/j.rser.2012.02.051.

[20] Feng, Q. G., Lin, Q. Y., Yu, Q. J., Zhao, S. Y., Yang, L. F., & Sugita, S. (2004). Concrete with highly active rice husk ash. Journal Wuhan University of Technology, Materials Science Edition, 19(3), 74–77. doi:10.1007/bf02835067.

[21] Padhi, R. S., Patra, R. K., Mukharjee, B. B., & Dey, T. (2018). Influence of incorporation of rice husk ash and coarse recycled concrete aggregates on properties of concrete. Construction and Building Materials, 173, 289–297. doi:10.1016/j.conbuildmat.2018.03.270.

[22] Prasara-A, J., & Gheewala, S. H. (2017). Sustainable utilization of rice husk ash from power plants: A review. Journal of Cleaner Production, 167, 1020–1028. doi:10.1016/j.jclepro.2016.11.042.

[23] Huang, H., Gao, X., Wang, H., & Ye, H. (2017). Influence of rice husk ash on strength and permeability of ultra-high performance concrete. Construction and Building Materials, 149, 621–628. doi:10.1016/j.conbuildmat.2017.05.155.

[24] Arabani, M., & Tahami, S. A. (2017). Assessment of mechanical properties of rice husk ash modified asphalt mixture. Construction and Building Materials, 149, 350–358. doi:10.1016/j.conbuildmat.2017.05.127.

[25] Le, H. T., & Ludwig, H. M. (2020). Alkali silica reactivity of rice husk ash in cement paste. Construction and Building Materials, 243, 118145. doi:10.1016/j.conbuildmat.2020.118145.

[26] Camargo-Pérez, N. R., Abellán-García, J., & Fuentes, L. (2023). Use of rice husk ash as a supplementary cementitious material in concrete mix for road pavements. Journal of Materials Research and Technology, 25, 6167–6182. doi:10.1016/j.jmrt.2023.07.033.

[27] Chalee, W., Sasakul, T., Suwanmaneechot, P., & Jaturapitakkul, C. (2013). Utilization of rice husk-bark ash to improve the corrosion resistance of concrete under 5-year exposure in a marine environment. Cement and Concrete Composites, 37(1), 47–53. doi:10.1016/j.cemconcomp.2012.12.007.

[28] Zain, M. F. M., Islam, M. N., Mahmud, F., & Jamil, M. (2011). Production of rice husk ash for use in concrete as a supplementary cementitious material. Construction and Building Materials, 25(2), 798–805. doi:10.1016/j.conbuildmat.2010.07.003.

[29] Makul, N., & Sua-iam, G. (2018). Effect of granular urea on the properties of self-consolidating concrete incorporating untreated rice husk ash: Flowability, compressive strength and temperature rise. Construction and Building Materials, 162, 489–502. doi:10.1016/j.conbuildmat.2017.12.023.

[30] Hwang, C. L., & Huynh, T. P. (2015). Effect of alkali-activator and rice husk ash content on strength development of fly ash and residual rice husk ash-based geopolymers. Construction and Building Materials, 101, 1–9. doi:10.1016/j.conbuildmat.2015.10.025.

[31] Nuaklong, P., Janprasit, K., & Jongvivatsakul, P. (2021). Enhancement of strengths of high-calcium fly ash geopolymer containing borax with rice husk ash. Journal of Building Engineering, 40, 102762. doi:10.1016/j.jobe.2021.102762.

[32] Patil, G. M., & Prakash, S. S. (2024). Effect of macro-synthetic and hybrid fibres on the behaviour of square concrete columns reinforced with GFRP rebars under eccentric compression. Structures, 59, 105707. doi:10.1016/j.istruc.2023.105707.

[33] Nematzadeh, M., & Fallah-Valukolaee, S. (2021). Experimental and analytical investigation on structural behavior of two-layer fiber-reinforced concrete beams reinforced with steel and GFRP rebars. Construction and Building Materials, 273, 121933. doi:10.1016/j.conbuildmat.2020.121933.

[34] Yoo, D. Y., Kwon, K. Y., Park, J. J., & Yoon, Y. S. (2015). Local bond-slip response of GFRP rebar in ultra-high-performance fiber-reinforced concrete. Composite Structures, 120, 53–64. doi:10.1016/j.compstruct.2014.09.055.

[35] Yoo, D. Y., Banthia, N., & Yoon, Y. S. (2016). Flexural behavior of ultra-high-performance fiber-reinforced concrete beams reinforced with GFRP and steel rebars. Engineering Structures, 111, 246–262. doi:10.1016/j.engstruct.2015.12.003.

[36] Sijavandi, K., Sharbatdar, M. K., & Kheyroddin, A. (2021). Experimental evaluation of flexural behavior of High-Performance Fiber Reinforced Concrete Beams using GFRP and High Strength Steel Bars. Structures, 33, 4256–4268. doi:10.1016/j.istruc.2021.07.020.

[37] Banthia, N., & Gupta, R. (2006). Influence of polypropylene fiber geometry on plastic shrinkage cracking in concrete. Cement and Concrete Research, 36(7), 1263–1267. doi:10.1016/j.cemconres.2006.01.010.

[38] Celik, K., Meral, C., Mancio, M., Mehta, P. K., & Monteiro, P. J. M. (2014). A comparative study of self-consolidating concretes incorporating high-volume natural pozzolan or high-volume fly ash. Construction and Building Materials, 67, 14–19. doi:10.1016/j.conbuildmat.2013.11.065.

[39] Celik, K., Jackson, M. D., Mancio, M., Meral, C., Emwas, A. H., Mehta, P. K., & Monteiro, P. J. M. (2014). High-volume natural volcanic pozzolan and limestone powder as partial replacements for portland cement in self-compacting and sustainable concrete. Cement and Concrete Composites, 45, 136–147. doi:10.1016/j.cemconcomp.2013.09.003.

[40] Kotynia, R., Szczech, D., & Kaszubska, M. (2017). Bond Behavior of GRFP Bars to Concrete in Beam Test. Procedia Engineering, 193, 401–408. doi:10.1016/j.proeng.2017.06.230.

[41] Meraz, M. M., Sobuz, Md. H. R., Mim, N. J., Ali, A., Islam, Md. S., Safayet, Md. A., & Mehedi, Md. T. (2023). Using rice husk ash to imitate the properties of silica fume in high-performance fiber-reinforced concrete (HPFRC): A comprehensive durability and life-cycle evaluation. Journal of Building Engineering, 76, 107219. doi:10.1016/j.jobe.2023.107219.

[42] Jittin, V., & Bahurudeen, A. (2022). Evaluation of rheological and durability characteristics of sugarcane bagasse ash and rice husk ash based binary and ternary cementitious system. Construction and Building Materials, 317, 125965. doi:10.1016/j.conbuildmat.2021.125965.

[43] Pachla, E. C., Silva, D. B., Stein, K. J., Marangon, E., & Chong, W. (2021). Sustainable application of rice husk and rice straw in cellular concrete composites. Construction and Building Materials, 283, 122770. doi:10.1016/j.conbuildmat.2021.122770.

[44] Zhu, H., Zhai, M., Liang, G., Li, H., Wu, Q., Zhang, C., & Hua, S. (2021). Experimental study on the freezing resistance and microstructure of alkali-activated slag in the presence of rice husk ash. Journal of Building Engineering, 38, 102173. doi:10.1016/j.jobe.2021.102173.

[45] El-Sayed, T. A., & Algash, Y. A. (2021). Flexural behavior of ultra-high performance geopolymer RC beams reinforced with GFRP bars. Case Studies in Construction Materials, 15, e00604. doi:10.1016/j.cscm.2021.e00604.

[46] Carrillo, J., Calixto-Vargas, J., & Burgos, E. A. (2024). Shear behavior of concrete panels reinforced with GFRP bars under cyclic diagonal tension tests. Engineering Structures, 302, 117340. doi:10.1016/j.engstruct.2023.117340.

[47] Vinod Kumar, M., Siddaramaiah, Y. M., & Jebamalai Raj, S. (2022). Shear behaviour of GFRP retrofitted spiral transverse reinforced concrete beams with partially replaced recycled aggregates. Materials Today: Proceedings, 65, 1642–1650. doi:10.1016/j.matpr.2022.04.700.

[48] Ali, H., Assih, J., & Li, A. (2021). Flexural capacity of continuous reinforced concrete beams strengthened or repaired by CFRP/GFRP sheets. International Journal of Adhesion and Adhesives, 104, 102759. doi:10.1016/j.ijadhadh.2020.102759.

[49] Prasad, R., & Pandey, M. (2012). Rice Husk Ash as a Renewable Source for the Production of Value Added Silica Gel and its Application: An Overview. Bulletin of Chemical Reaction Engineering & Catalysis, 7(1), 1–25. doi:10.9767/bcrec.7.1.1216.1-25.

[50] Real, C., Alcala, M. D., & Criado, J. M. (1996). ChemInform Abstract: Preparation of Silica from Rice Husks. ChemInform, 27(49). doi:10.1002/chin.199649266.

[51] Liou, T. H., & Yang, C. C. (2011). Synthesis and surface characteristics of nanosilica produced from alkali-extracted rice husk ash. Materials Science and Engineering: B, 176(7), 521–529. doi:10.1016/j.mseb.2011.01.007.

[52] ASTM C192/C192M-19.(2024). Standard Practice for Making and Curing Concrete Test Specimens in the Laboratory. ASTM International, Pennsylvania, United States. doi:10.1520/C0192_C0192M-19.

[53] Gerges, N. N., Issa, C. A., & Fawaz, S. (2015). Effect of construction joints on the splitting tensile strength of concrete. Case Studies in Construction Materials, 3, 83–91. doi:10.1016/j.cscm.2015.07.001.

[54] ACI Committee 318. (2019). ACI 318-19: Building Code Requirements for Structural Concrete (ACI 318-19) and Commentary (ACI 318R-19). American Concrete Institute, Michigan, United States.

[55] Chou, J. S., Liu, C. Y., Prayogo, H., Khasani, R. R., Gho, D., & Lalitan, G. G. (2022). Predicting nominal shear capacity of reinforced concrete wall in building by metaheuristics-optimized machine learning. Journal of Building Engineering, 61, 10504. doi:10.1016/j.jobe.2022.105046.

[56] Bixapathi, G., & Saravanan, M. (2022). Strength and durability of concrete using Rice Husk ash as a partial replacement of cement. Materials Today: Proceedings, 52, 1606–1610. doi:10.1016/j.matpr.2021.11.267.

[57] Nasir Amin, M., Ur Rehman, K., Shahzada, K., Khan, K., Wahab, N., & Abdulalim Alabdullah, A. (2022). Mechanical and microstructure performance and global warming potential of blended concrete containing rice husk ash and silica fume. Construction and Building Materials, 346, 128470. doi:10.1016/j.conbuildmat.2022.128470.

[58] Díaz, A. G., Bueno, S., Villarejo, L. P., & Eliche-Quesada, D. (2024). Improved strength of alkali activated materials based on construction and demolition waste with addition of rice husk ash. Construction and Building Materials, 413, 134823. doi:10.1016/j.conbuildmat.2023.134823.

[59] Onyenokporo, N. C., Taki, A., Montalvo, L. Z., & Oyinlola, M. (2023). Thermal performance characterization of cement-based masonry blocks incorporating rice husk ash. Construction and Building Materials, 398, 132481. doi:10.1016/j.conbuildmat.2023.132481.

[60] Rahimi, M. Z., Zhao, R., Sadozai, S., Zhu, F., Ji, N., & Xu, L. (2023). Research on the influence of curing strategies on the compressive strength and hardening behaviour of concrete prepared with Ordinary Portland Cement. Case Studies in Construction Materials, 18, 2045. doi:10.1016/j.cscm.2023.e02045.

[61] Al-Amoudi, O. S. B., Maslehuddin, M., Ibrahim, M., Shameem, M., & Al-Mehthel, M. H. (2011). Performance of blended cement concretes prepared with constant workability. Cement and Concrete Composites, 33(1), 90–102. doi:10.1016/j.cemconcomp.2010.10.004.

[62] Liu, S., Zhou, Y., Zhou, J., Zhang, B., Jin, F., Zheng, Q., & Fan, H. (2019). Blast responses of concrete beams reinforced with GFRP bars: Experimental research and equivalent static analysis. Composite Structures, 226, 111271. doi:10.1016/j.compstruct.2019.111271.

[63] Doostmohamadi, A., Shakiba, M., Bazli, M., Ebrahimzadeh, M., & Arashpour, M. (2023). Enhancement of bond characteristics between sand-coated GFRP bar and normal weight and light-weight concrete using an innovative anchor. Engineering Structures, 294, 116780. doi:10.1016/j.engstruct.2023.116780.

[64] Manoj, T., Mrudhul varma, B., & Seshagiri rao, M. V. (2023). Performance evaluation of conventional and lightweight concrete using GFRP sheets at elevated temperature. Materials Today: Proceedings, 1-7. doi:10.1016/j.matpr.2023.05.115.

[65] Doostmohamadi, A., Karamloo, M., & Afzali-Naniz, O. (2020). Effect of polyolefin macro fibers and handmade GFRP anchorage system on improving the bonding behavior of GFRP bars embedded in self-compacting lightweight concrete. Construction and Building Materials, 253, 119230. doi:10.1016/j.conbuildmat.2020.119230.

[66] Yang, X., Liu, Y., Wang, Y. F., & Zhang, J. (2024). Performance of steel tube reinforced concrete-filled weathering steel tubular members under lateral impact loading. Journal of Constructional Steel Research, 213, 108382. doi:10.1016/j.jcsr.2023.108382.

[67] Zheng, Y., Su, Z., Li, J., Wang, Z., Xu, Y., Li, X., & Che, P. (2024). Energy transfer efficiency and rock damage characteristics of a hydraulic impact hammer with different tool shapes. International Journal of Impact Engineering, 188, 104933. doi:10.1016/j.ijimpeng.2024.104933.

[68] Cai, X., Zhang, X., Lu, Y., Noori, A., Han, S., & Chen, L. (2024). A novel braided bamboo composite material with balanced strength and good energy absorption capacity inspired by bamboo. Construction and Building Materials, 421, 135652. doi:10.1016/j.conbuildmat.2024.135652.

[69] Mou, B., Liu, X., Zhao, O., & Xiao, H. (2023). Dynamic response of concrete-filled square steel tubular columns under lateral impact load at flat or corner zone. Engineering Structures, 292, 116319. doi:10.1016/j.engstruct.2023.116319.

[70] Mostofinejad, D., Aghamohammadi, O., Bahmani, H., & Ebrahimi, S. (2023). Improving thermal characteristics and energy absorption of concrete by recycled rubber and silica fume. Developments in the Built Environment, 16, 100221. doi:10.1016/j.dibe.2023.100221.

[71] Alam, A., & Hu, J. (2023). Mechanical properties and energy absorption capacity of plain and fiber-reinforced single- and multi-layer cellular concrete. Construction and Building Materials, 394, 132154. doi:10.1016/j.conbuildmat.2023.132154.

[72] Kumar, V., Iqbal, M. A., & Mittal, A. K. (2018). Study of induced prestress on deformation and energy absorption characteristics of concrete slabs under drop impact loading. Construction and Building Materials, 188, 656–675. doi:10.1016/j.conbuildmat.2018.08.113.